# A transmission grating pulse stretcher for contrast enhancement of Gemini

**Contact** *yunxin.tang@stfc.ac.uk*

**Yunxin Tang, Chris Hooker, Oleg Chekhlov, Steve Hawkes, John Collier and P. P. Rajeev**

*Central Laser Facility,*
*STFC Rutherford Appleton Laboratory,*
*Didcot, Oxon OX11 0QX, UK*

## Introduction

With recent progress in chirped pulse amplification (CPA) [1] technology, extreme laser power and intensity as high as ~$10^{22}$ W/cm$^2$ has been made available by the new generation Petawatt (PW) class Ti:Sapphire amplifiers with an ultrashort pulse duration of around 30fs [2-7]. Ultra-high intensity lasers have proved to be a very powerful and efficient drive source to accelerate electrons to multi-GeV energies. Such lasers can also be used to accelerate protons to generate multi-MeV proton beams with high brightness and low emittance, paving the way towards compact sources for cancer therapy. There is also increasing interest in using ultra-intense lasers for high harmonic generation from solid density plasma to produce sub-femtosecond coherent XUV/x-ray pulses with extreme brightness. The temporal contrast of the laser pulses plays a crucial role in these high field laser-matter interaction experiments [8-10]. Clean and high temporal quality laser pulses are essential to restrict any destructive preplasma dynamics, as excessive prepulse intensity can significantly modify, damage or even destroy the solid state targets due to formation of a preplasma prior to the arrival of the main pulse [11-13]. For these reasons, many workers have devoted significant effort to improving the contrast of CPA laser pulses.

However, improving the contrast within 10-20ps of the main pulse peak has proven to be extremely challenging for the high power laser community. Some improvement of the contrast within 1 picosecond has been demonstrated by means of precise spectral control [14]. Our previous investigation of contrast in an ultrashort pulse high power Ti:Sapphire laser system showed that the second grating of the pulse stretcher is the major source of the triangular feature in the compressed pulse temporal profile, known as the contrast pedestal [15]. In this paper we propose for the first time a novel pulse stretcher for high power lasers made using two transmission gratings, and demonstrate its superiority in terms of pulse temporal quality over conventional stretchers employing reflective gratings. We have investigated the contrast pedestal of such a stretcher compared with a conventional gold grating stretcher with the same stretching factor, and have obtained more than an order of magnitude reduction in the contrast pedestal.

## 2. System description and research background

We used the front end of the Gemini laser for these tests. A detailed description of Gemini can be found elsewhere [15]. The front end consists of an oscillator followed by a kHz preamplifier whose output is a train of pulses at the mJ level, stretched to around 7 picoseconds by material dispersion. A train of pulses at 10 Hz is switched into the main amplifier chain, and the remaining pulses from the kHz train were used in the work described here. Fig.1 shows a typical temporal profile of the compressed Gemini laser pulse measured recently. There are three distinct features in the temporal profile: 1) the platform of amplified spontaneous emission (ASE) somewhat below $10^{-10}$ of peak intensity extending over many nanoseconds; 2) various discrete pre- and post-pulses in the range of a few of hundreds of picoseconds; and 3) a triangularly shaped feature occupying the ~20 picoseconds either side of the main pulse peak, known as the contrast pedestal (CP). The discrete pre-pulses were converted from their counterpart post-pulses, generated by internal reflections in the optical components in the laser chain, through non-linear processes associated with B-integral [16]. These can be reduced or eliminated by changes to optical components, such as improved anti-reflection coatings, Brewster-angled windows and introducing wedges (matched to avoid angular dispersion). The ASE can be reduced by techniques such as XPW [17] and improving the extinction ratio of Pockels cells used for pulse selection. However, none of these techniques has any effect on the contrast pedestal. This feature, which appears in some form in almost all high-power CPA lasers, is a major obstacle to achieving the highest possible contrast. In this paper we report on recent significant progress in addressing this long-standing problem.

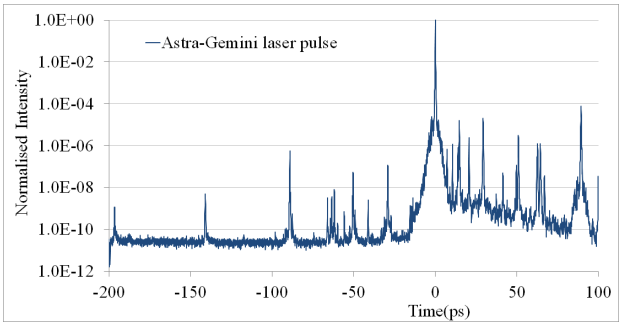


Fig. 1. Typical temporal profiles of Astra-Gemini laser pulses

In our previous study, we evaluated the effect of each individual optical component in the stretcher on the contrast of the compressed laser pulses, and found that the gold gratings in the stretcher are mainly responsible for the contrast pedestal. Gratings can influence the temporal profile of the pulse when scattering and surface irregularities introduce spectral phase noise in a spatially dispersed beam [15]. Theoretical work has shown that spectral phase noise in the dispersed beam can cause exponential profiles in the time domain with a form similar to that of the contrast pedestal [18]. We demonstrated that the contrast pedestal was reduced by an order of magnitude when the original photoresist second grating was replaced by an etched grating of higher quality.

The surface irregularities and roughness of gold gratings arise from the manufacturing process, in which the underlying periodic structure is formed either directly as an exposed photoresist layer or by etching the grating substrate. Developed photoresist has some small-scale roughness, as can be seen in scanning electron microscope (SEM) pictures of such gratings. A grating formed by etching the substrate surface is inherently

smoother, but both types must be coated with gold, and the coating process can introduce additional roughness, as it is difficult to apply a coating that is fully conformal with the groove structure. If the etched substrate is left uncoated, the result is a transmission grating. SEM images of such gratings show an extremely clean, smooth and precisely defined groove structure [19]. This suggests that using etched transmission gratings in the stretcher could minimize the effects of grating surface roughness on the spectral phase noise, and hence reduce the level of the contrast pedestal.

Transmission gratings have an added advantage: roughness levels in a transmission grating will generate a smaller amount of spectral phase noise than the same roughness in a reflection grating, because light undergoes a much smaller phase change in transmission, compared to reflection. Along the dispersion direction, the optical frequency ω and position x in the spatially dispersed beam are related by x = g(ω). For a given grating surface roughness profile z(x), we get z(x) = z(g(ω)) = Z(ω). For a reflection grating, the spectral phase noise $\delta\varphi_g(\omega)$ is given by:

$$\delta\varphi_g(\omega) = \frac{4\pi}{\lambda} Z(\omega) \quad , \qquad (1)$$

whereas the spectral phase noise $\delta\varphi_t(\omega)$ for a transmission grating is given by:

$$\delta\varphi_t(\omega) = \frac{2\pi(n-1)}{\lambda} Z(\omega) \quad , \qquad (2)$$

where λ denotes the wavelength and n the refractive index of the transmission grating substrate. As (n-1) is approximately 0.5 for most commonly used substrate materials, $\delta\varphi_g(\omega)/\delta\varphi_t(\omega)$ will have a value close to 4. Our previous contrast study showed that smooth, optically polished surfaces in the stretcher, i.e. the mirrors, make a negligible contribution to the contrast pedestal. Since the back surface of the transmission grating is a high quality flat optical surface, it will introduce a negligible amount of spectral phase error. This suggests that a transmission grating should introduce four times less spectral phase noise than a reflection grating, and that a pulse stretcher made using transmission gratings would significantly reduce the level of the contrast pedestal.

## 3. Experimental Study

### *3.) The effect of the first grating*

Every stretcher has two gratings, which contribute differently to the pedestal because the beam is undispersed on the first and dispersed on the second. To distinguish the effects of dispersion and stretching, in our previous work we investigated the effect of the first gold grating on the contrast pedestal. We subsequently examined the effect of a single transmission grating in a similar way (see Ref 15 for the schematic of the non-stretching geometry), using a standard transmission grating obtained from Ibsen Photonics A/S. The transmission grating was positioned at the centre of curvature of a spherical mirror of radius 750mm. Pulses from a kHz femtosecond source, slightly stretched to ~7 ps by material dispersion, were dispersed by the grating and retro-reflected back to the same point on the grating by the curved mirror. The input and output beams on the grating were at conjugate image points, and hence each individual wavelength propagated through exactly the same optical path, resulting in no stretching of the pulse. The output beam was sent through a pair of prisms to be compressed to an ultrashort pulse of near transform-limit, and the temporal contrast of the compressed pulse was then measured with a commercial 3rd order auto-correlator (Sequoia, Amplitude Technologies). The result is shown in Fig.2. The blue curve was obtained with the single gold grating, and the red curve with the single transmission grating. It is clear that the transmission grating introduces a shorter and smaller contrast pedestal, in particular when approaching the wing, compared with the gold grating. This supports our conclusion above that transmission gratings would be superior to gold gratings in terms of contrast, and prompted a more thorough investigation, detailed below, evaluating the effect on the contrast pedestal of a complete transmission grating stretcher.

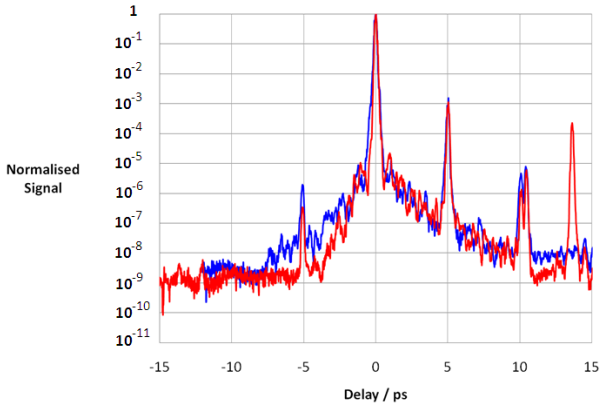


Fig. 2. Effect of first transmission grating on contrast pedestal

### *3.2) The effect of a full transmission grating stretcher*

In order to fully understand and evaluate the advantage of transmission gratings over reflective gratings in regard to the contrast pedestal, we designed and constructed a test transmission grating stretcher and a corresponding reflective grating compressor. The configuration of the transmission grating stretcher was based on a similar concept to that of the Gemini laser, but on a smaller scale and hence with a smaller stretching factor, limited by the largest size of transmission grating commercially available. The geometry of the stretcher was developed independently at the Central Laser Facility [20], and is different from the conventional Martinez [21] and Öffner stretcher configurations [22]. Nevertheless, high power laser systems elsewhere that use Öffner or other types of stretcher all exhibit a similar contrast pedestal in their pulses after compression, so the details of the stretcher geometry do not appear to be important for generating the pedestal.

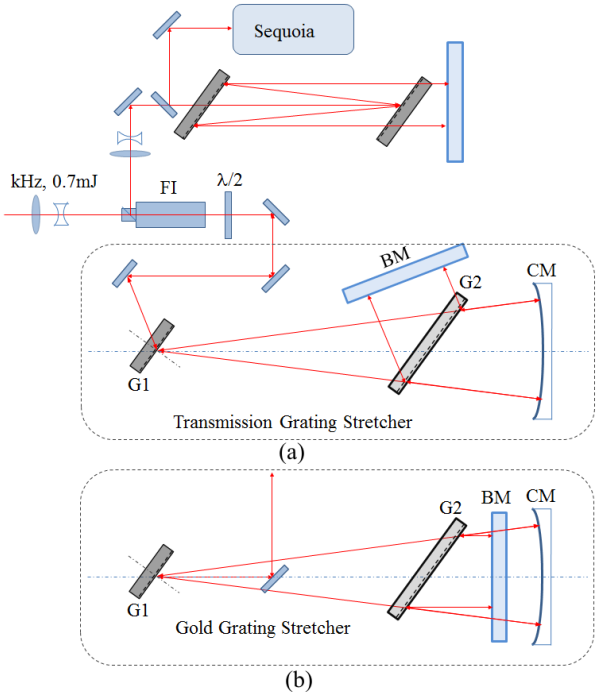


Fig. 3. Schematic of a) transmission grating stretcher and gold grating compressor set-up, G1 and G2: transmission gratings; CM: curved mirror; BM: back mirror; and FI: Faraday Isolator; b) gold grating stretcher.

The schematic of the experimental set up is shown in Figure 3. The source beam is a kHz train of unstretched laser pulses,

with ~7ps pulse duration at ~0.7mJ from a commercial Ti:Sa amplifier (Femtolasers). As shown in Figure 3, the input laser pulses were injected into the transmission grating stretcher though a Faraday Isolator (FI). The dispersed beam passed above G2 initially, then after reflection from the curved mirror it was incident on the top of G2 and deflected to the back mirror (BM), before returning along the same path. The output beam was separated from the input beam on its return to the input polarizer of the FI due to the orthogonal polarisation. The stretched laser pulse was spatially expanded and collimated by a telescope to a larger beam size, and then sent into the gold grating compressor. Unlike the gold gratings, the transmission gratings have TE polarisation orientation for optimum diffraction efficiency. As the stretcher was arranged in the in-plane configuration while the compressor was in the out-of-plane geometry, the polarisation orientations of stretcher and compressor were orthogonal to each other, as defined by the polarizer at the entrance of the isolator, thus no polarization rotation components were needed between the stretcher and compressor. The stretched pulse was recompressed to near the transform limit by the compressor, in conjunction with a Dazzler to compensate for the residual high order phase. The setup had an overall passive transmission of around 40%, so after the compressor the beam had to be demagnified with a reflective telescope to achieve the intensity necessary to measure the contrast with high dynamic range. The contrast of the compressed laser pulse was measured with a Sequoia, as before.

The transmission gratings used for the test have a groove density of 1480 lines/mm, which is the same as the full size reflective stretcher of the Gemini laser. They were set at 36.3°, the Littrow angle at the central wavelength of 800nm in the stretcher. The first transmission grating was placed at the centre of curvature of the spherical mirror, and the two gratings were separated by an axial distance of ~250mm, corresponding to a nominal grating separation of ~202mm. This resulted in a stretched pulse length of ~160ps for the available spectral bandwidth, compared with the stretched pulse length of ~520ps provided by the full size stretcher of Gemini. The stretch factor of the transmission grating stretcher was limited by the ruled dimension of the second transmission grating, which was only 70mm x 10mm. This was the largest customized transmission grating available from the commercial supplier, Ibsen Photonics A/S. Nevertheless, we expected the comparison between similar transmission- and reflection-grating stretchers to give a representative result that would indicate the potential of a full-sized transmission grating stretcher for reducing the contrast pedestal.

A pair of gold gratings was used to build the compressor to recompress the stretched pulses. Unfortunately, the only available gratings had a groove density of 1500 lines/mm, slightly different from the 1480 lines/mm of the transmission gratings in the stretcher. We were concerned that the excessive residual high order phase due to the grating line density mismatch would significantly affect the compression close to the main peak, and lead to uncertainty in the true value of the pulse contrast. To evaluate this we carried out a detailed dispersion analysis, taking into account the dispersion of the ~48mm of Terbium Gallium Garnet (TGG) in the Faraday rotator, to assess the effect of the grating line density mismatch on the compressed pulse. Assuming that the non-dispersive angle for the stretcher is ~3.5°, the transmission gratings in the stretcher were set at the Littrow angle of 36.378° and separated by a nominal distance of ~202mm, giving a stretched pulse length of ~160ps. Assuming that the non-dispersive angle for the compressor input and output beam are 3.5°and 4°, respectively, we started the analysis by setting the compressor gratings at the Littrow angle of 36.95° and adjusting the grating separation to 192.9mm for the minimum overall group delay. There exists a huge spectral phase error at this point with a residual second order phase (GVD) of 1690fs$^2$, third order phase (TOD) of 117.8x10$^3$fs$^3$ and fourth order phase (FOD) of -9.2x10$^5$fs$^4$. Optimisation was carried out by changing the incident angle into the compressor and adjusting the grating separation accordingly to minimise the overall group delay. We found that if the incidence angle into the compressor is increased to 38.1045°, with a nominal grating separation of 201.7812mm, the optimised overall group delay and relatively flat residual spectral phase are obtained. Fig. 4 shows the calculated overall group delay and corresponding spectral phase error at the optimum settings due to the grating line density mismatch and material dispersion in TGG. As can be seen, both GVD (~ 3.5fs$^2$) and TOD (~ 134fs$^3$) are almost zero, with only a small amount of remaining FOD at a value of about ~ 9.7x10$^4$ fs$^4$. The simulation result indicated clearly that the high order phase error introduced by a small grating line density mismatch would be negligible when the beam incident angle into the compressor was increased slightly with a correspondingly larger separation. In principle, therefore, the stretched pulse could be compressed to a short pulse of near transform limit within the spectral bandwidth concerned in this investigation, without introducing any degradation in the contrast pedestal even in the presence of a small grating line density mismatch.

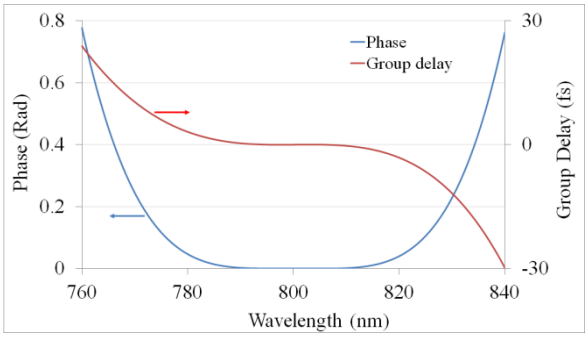


Fig. 4. Calculated spectral phase in the presence of grating line density mismatch.

In order to minimise the aberration and hence the additional phase error introduced by the optics in the stretcher, the beam size into the stretcher was kept small, in the range of a fraction of a millimetre. Since the focal length of the curved mirror in the testing stretcher is relatively short at 375mm and the separation of two gratings is only one third of the curved mirror radius, it was quite difficult to maintain a good match of the input laser beam spatial profile with the natural spatial mode of the stretcher. A great deal of care was taken to reshape and reformat the input beam to a suitable and correct beam size on the first grating. The output beam was carefully maintained to be almost the ideal -1:1 conjugate image of the input beam on the first grating to minimise the aberration and phase error induced when the stretcher was set-up. The gratings in both the stretcher and compressor were carefully aligned and optimised by monitoring the far field image. In particular, the parallelism of the grating planes in the main dispersion direction and the groove orientation direction were optimised by precisely overlapping two individual far field images of the wings of the laser pulse spectrum while the central section of the spectrum was blocked. By implementing this so-called two-colour method, the residual angular dispersion caused by a minor misalignment of the gratings was minimised, and estimated to be smaller than ~10μrad/nm for the stretcher and ~1μrad/nm for the compressor, respectively.

One of major objectives in this investigation was to directly compare the transmission gratings with gold gratings with regard to their effect on the contrast pedestal. To achieve this, a second stretcher was built using nearly identical geometry but with two gold gratings. Details of the alignment and optimization of this stretcher are essentially the same as for the transmission grating version. The stretched pulse was

recompressed by the same compressor, and the contrast measurement was carried out using the same third-order auto-correlator.

## 4. Results and discussion

The compressed pulses were characterized and monitored by a commercial FROG instrument (Grenouille). The pulse compression was optimised by changing the incident angle into the compressor and making a corresponding change in the grating separation, in conjunction with adjustments of the Dazzler settings to compensate the residual high order phase due to the grating line density mismatch and the material dispersion in the system. A typical retrieved pulse shape and FROG trace for optimised compressed pulses are shown in Fig. 5, where the solid line denotes the measured pulse intensity, the dotted line the calculated transform limited pulse and the dashed line the measured phase in the time domain. Fig. 5 shows clearly that a near transform-limited short pulse was obtained with a duration of ~35fs, which is good enough to ensure a reliable contrast measurement. The temporal profile of the compressed pulses was measured with the Sequoia.

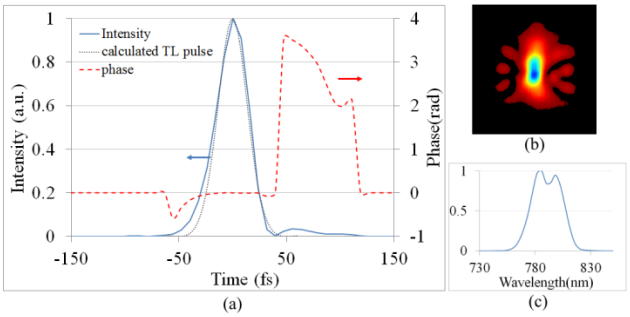


Fig. 5. a) Retrieved pulse and phase, b) FROG trace of the compressed pulse and c) the spectrum

After fully characterising the compressed pulses obtained from the transmission grating stretcher, the transmission gratings in the stretcher were replaced by a pair of reflective gratings with the same line density as the compressor gratings. The gold gratings in the stretcher are placed at the Littrow angle of ~36.9° and separated by an axial distance of ~244mm, slightly different from the parameters of transmission grating stretcher but giving the same stretched pulse length of ~160ps for the available spectral bandwidth. This near identical gold grating stretcher as shown in Fig. 3(b) was set up to have the same stretching factor as that of the transmission grating stretcher. It was again carefully aligned up and optimised by the method of 2 colours in the far field as described above. The stretched pulse was recompressed by the same compressor to a near transform limited short pulse of ~32fs, and a FROG trace that was indistinguishable from the one shown in Fig.5. The temporal profile of the compressed pulse was measured with the Sequoia, as before.

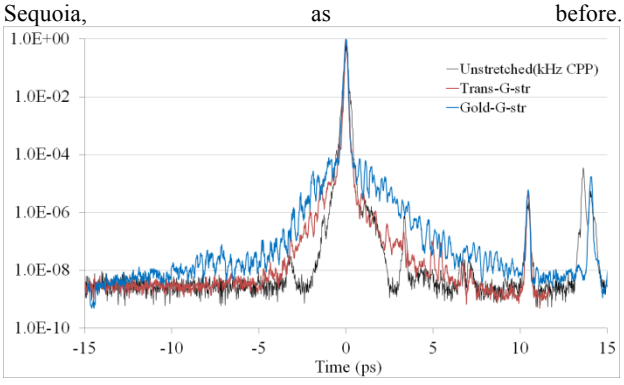


Fig. 6. The contrast measurement of transmission grating stretcher (red) and gold grating stretcher (blue).

Fig.6 presents the comparison of contrast traces using the transmission grating-based (red) and reflective grating based (blue) stretchers. It is clear that the contrast pedestal induced by the transmission grating stretcher is between 1 and 2 orders of magnitude smaller than that from the reflective grating stretcher. This is a significant improvement in the pulse contrast close to the main peak, and clearly demonstrates the superior performance of the transmission grating stretcher relative to the reflective grating stretcher, with regard to the contrast pedestal.

We notice that there is still a significant residual contrast pedestal associated with the transmission grating stretcher, compared with the seed pulse. This residual contrast pedestal is larger than we would expect from the superior surface quality of the transmission gratings. It is possible that the gold gratings of the compressor could give rise to a contrast pedestal on the compressed pulse, as the beam size through the compressor was relatively small at ~7mm. In our previous paper we showed that the compressor gratings in Gemini make a negligible contribution to the contrast pedestal, because the beam diameter is large enough (150mm) to average out the effect of spectral phase noise induced by the gratings [15]. Where the beam is small, as is the case in the pulse stretcher, irregularities on the gratings do introduce significant spectral phase noise, and this will also occur in pulse compressors if the beam size is too small [23]. We therefore anticipate that the advantage of the transmission gratings would be fully exploited, and a greater improvement in the contrast pedestal be achieved, by implementing a full-scale transmission grating stretcher for Gemini. We are planning to construct and test such a stretcher in the near future.

## 5. Grating surface characterization

In order to understand the effect of spectral phase noise induced by the grating surface roughness on the contrast pedestal in more detail, we quantitatively characterised the surface quality of the transmission and gold gratings used in the experiments by measuring the surface roughness. We measured the grating surface profiles using a commercial interferometer, a ZYGO XP/D with a 4-inch aperture. When used at the largest possible magnification, the interferogram can reveal the fine structure of the surface quality over an area of up to ~70mm, covering the full length of the second gratings in the stretcher, with a spatial resolution of 70 to 100 microns.

It is well known that a modulation of $\Delta\nu$ in the frequency domain is associated with a characteristic time or a replica peak at $\pm\tau$ in the time domain, governed by $\Delta\nu \times \tau \sim 1$. This characteristic time is therefore related to a corresponding spatial structure of surface roughness on the second grating, placed at the Littrow angle in the stretcher, where the beam is spatially dispersed. The periodicity of this corresponding spatial structure can be estimated by:

$$\delta x \approx \frac{L_0 N}{1-\left(\frac{N\lambda_0}{2}\right)^2}\frac{1}{\tau}\frac{\lambda_0^2}{c} \quad , \tag{3}$$

where $\delta x$ is the wavelength of the spatial structure, $L_0$ the grating separation on axis, N the grating line density, $\tau$ the time range under investigation, $\lambda_0$ the central wavelength of the laser pulse and c the light speed. The smaller the structure on the grating surface, the larger the characteristic time it will induce. Therefore, $\delta x$ approximately defines the minimum spatial resolution required for the grating surface measurement for a time range of $\tau$ under investigation. For instance, we are interested in the contrast profile spanning over ~ 5ps around the main peak, which corresponds to a minimum spatial structure of ~250μm on the second grating, calculated by equation (3), in the case of experiment described above. The spatial resolution in our grating surface roughness measurement is much better

than this estimated minimum spatial structure, and hence it provides sufficient information on the spectral phase noise to maintain the fidelity of the contrast in future simulations.

Having obtained the grating surface profile, the spectral phase noise on the second grating in the stretcher, which is illuminated by the dispersed beam, is given by equation (1) for the gold grating and equation (2) for the transmission grating. The images in Fig. 7(a) and (c) show the measured grating surface profiles of gold and transmission gratings respectively, while the blue and red curves in Fig. 7(b) and (d) show a typical spectral phase noise distributions as a function of wavelength at the selected line across the grating surface. Since the beam interacts with the second grating twice in our stretcher, the spectral phase noise shown in Fig. 7 (b) and (d) is twice the values obtained from equations (1) and (2).

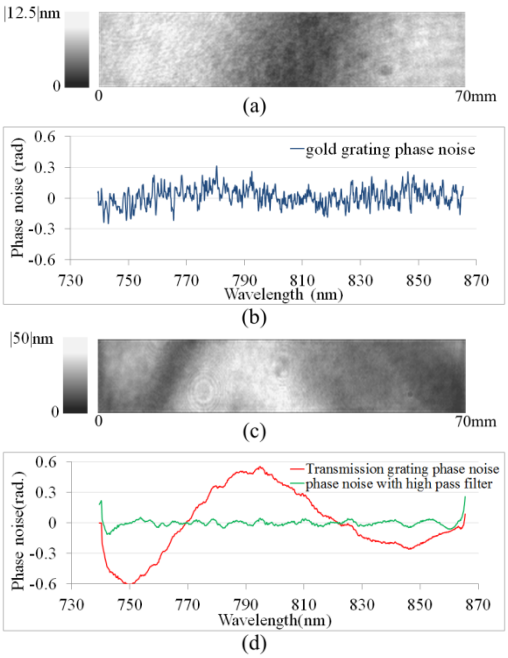


Fig. 7. Measured grating surface profiles: (a) gold grating and (b) typical phase noise at the central line; (c) transmission grating and (d) typical phase noise at the central line.

There are obvious differences between the spectral phase noise arising from the gold and transmission gratings, as shown in Fig. 7. The high-frequency phase noise present on the gold grating, which arises from the fine surface modulations, are virtually absent from the transmission grating. In contrast, the spectral phase of the transmission grating shows a relatively large but slow variation with wavelength, slightly modulated with ripples. This slow variation in the spectral phase is due to the thickness variation of the transmission grating substrate, which is still less than $\lambda/10$ per pass and well within the normal tolerance of optical elements. In addition, this slow variation in the frequency domain corresponds to a characteristic time scale of ~<30fs, which lies within the main peak of the laser pulse and hence has no effect on the contrast pedestal on picosecond timescales. Only the small scale fine structured ripples influence the contrast pedestal in the few picoseconds around the main pulse. We have used a high pass filter to remove the very low frequency component in the spectral phase noise of the transmission grating, and the outcome is shown as a green curve in Fig. 7 (d). This residual modulation is responsible for the contrast pedestal related to the transmission grating over the time range under investigation. Since high-frequency content is far smaller in the case of transmission grating, it produces a pedestal spanning a shorter temporal range compared to the reflective grating. The absence of high-frequency phase errors is the result of a better surface quality of the transmission grating; the depth resolution of the ZYGO interferometer is <0.1nm, which would be sufficient to reveal any small-scale high frequency modulations, if present. The higher surface quality of the transmission grating has also been validated by a white light interferometer with a very high spatial resolution at <200nm.

The peak-to-peak value of the spectral phase noise for the gold grating is ~0.56 radians with a standard deviation of 0.086, while the peak-to-peak value of the spectral phase noise with high pass filter for the transmission grating is only about ~0.115 radians with a standard deviation of 0.023. The phase noise from the transmission grating is thus about 4 times less than that from the gold grating, as expected from the discussion above. According to Ref 18, one order of magnitude of difference in the standard deviation of spectral phase noise resulted in more than 2 orders of magnitude of improvement in the contrast pedestal. In addition, the spectral phase noise of the gold grating contains higher frequency components than that of transmission grating, resulting in temporal spreading over a longer time range. Therefore, the combined influence of these two factors should result in an overall improvement in the contrast pedestal of transmission gratings by more than an order of magnitude, which is consistent with the experimental results described above. Although beyond the scope of the present paper, detailed modelling and simulation of the contrast related to the measured grating surface roughness profile is underway, and will be presented in a future publication.

## 6. Conclusions

We have investigated the effect on the contrast pedestal of a pulse stretcher built using transmission gratings, and compared it with the performance of a conventional reflective gold grating stretcher. We have demonstrated the superior performance of the transmission gratings over the reflective gratings, resulting in an enhancement of the contrast by 1-2 orders of magnitude in the vicinity of the main peak of the compressed pulse. We have also quantitatively characterized the roughness of the grating surfaces and estimated its impact on the contrast pedestal. This result should provide useful guidelines for future grating manufacturing and characterization for improved contrast pedestal. As mentioned above, the geometry of the stretcher used in this investigation differs from the conventional Öffner stretcher configuration. However, high power laser systems elsewhere that use Öffner or other types of stretcher exhibit a similar contrast pedestal in their pulses after compression, which suggests that the geometry of the stretcher does not significantly affect the appearance of the contrast pedestal. The results of the investigation described here should therefore be of great significance for all CPA-based high power lasers.

## References

1. D. Strickland and G. Mourou, “Compression of amplified chirped optical pulses,” Opt. Commun. 56, 219-221(1985).

2. S. W. Bahk, P. Rousseau, T. Planchon, V. Chvykov, G. Kalintchenko, A. Maksimchuk, G. A. Mourou, and V. Yanovsky, “Generation and characterization of the highest laser intensities ($10^{22}$ W/cm$^2$ ),” Opt. Lett. 29, 2837-2839 (2004).

3. G. A. Mourou, T. Tajima, and S. V. Bulanov, “Optics in the relativistic regime,” Rev. Mod. Phys. 78, 309-371 (2006).

4. K. Ertel, C. Hooker, S. J. Hawkes, B. T. Parry, and J. L. Collier , “ASE suppression in a high energy Titanium sapphire amplifier,” Opt. Express 16, 8039-8049 (2008).

5. S. Laux, F. Lureau,1 C. Radier, O. Chalus, F. Caradec, O. Casagrande, E. Pourtal, C. Simon-Boisson, F. Soyer, and P. Lebarny, “Suppression of parasitic lasing in high energy, high repetition rate Ti:sapphire laser amplifiers,” Opt. Lett. 37, 1913-1915 (2012).

6. Z. Wang, C. Liu, Z. Shen, Q. Zhang, H. Teng, and Z. Wei, “High-contrast 1.16 PW Ti:sapphire laser system combined with a doubled chirped-pulse amplification scheme and a femtosecond optical-parametric amplifier,” Opt. Lett. 36, 3194-3196 (2011).

7. J. H. Sung, S. K. Lee, T. J. Yu, T. M. Jeong, and J. Lee, "0.1 Hz 1.0 PW Ti:Sapphire laser," Opt. Lett. 35, 3021-3023 (2010).

8. D. Umstadter, "Review of physics and applications of relativistic plasmas driven by ultra-intense lasers," Phys. Plasma 8, 1774-1785 (2001).

9. A. Zhidkov, J. Koga, A. Sasaki, and M. Uesaka, "Radiation Damping Effects on the Interaction of Ultra-intense Laser Pulses with an Overdense Plasma," Phys. Rev. Lett. 88, 185002_1-185002_4 (2002).

10. B. Dromey, S. Cousens, S. Rykovanov, M. Yeung, D. Jung, D. C. Gautier, T. Dzelzainis, D. Kiefer, S. Palaniyppan, R. Shah, J. Schreiber, J. C. Fernandez, C. L. S. Lewis, M. Zepf, and B. M Hegelich, "Coherent synchrotron emission in transmission from ultrathin relativistic laser plasmas," New J. Phys. 15, 015025 (14pp) (2013).

11. D. Neely, P. Foster, A. Robinson, F. Lindau, O. Lundh, A. Persson, C.-G.Wahlström, and P. McKenna, "Enhanced proton beams from ultrathin targets driven by high contrast laser pulses," Appl. Phys. Lett. 89, 021502_1-021502_3 (2006).

12. S. P. D. Mangles, A. G. R. Thomas, M. C. Kaluza, O. Lundh, F. Lindau, A. Persson, Z. Najmudin, C-G. Wahlstrom, C. D. Murphy, C. Kamperidis, K. L. Lancaster, E. Divall, and K. Krushelnick, "Effect of laser contrast ratio on electron beam stability in laser wakefield acceleration experiments," Plasma Phys. Control. Fusion 48, B83-B90 (2006).

13. L. A. Gizzi, C. Benedetti, C. A. Cecchetti, G. D. Pirro, A. Gamucci, G. Gatti, A. Giulietti, D, Giulietti, P. Koester, L. Labate, T. Levato, N. Pathak, and F. Piastra, "Laser-Plasma Acceleration with FLAME and ILIL Ultraintense Lasers," Appl. Sci. 3, 559-580 (2013).

14. D. Kaganovich, J. R. Peñano, M. H. Helle, D. F. Gordon, B. Hafizi, and A. Ting, "Origin and control of the subpicosecond pedestal in femtosecond laser systems," Opt. Lett. 38, 3635-3638 (2013).

15. C. Hooker, Y. Tang, O. Chekhlov, J. Collier, E. Divall, K. Ertel, S. Hawkes, B. Parry and P. P. Rajeev, "Improving coherent contrast of petawatt laser pulses," Opt. Express 19, 2193-2203 (2011).

16. N. V. Didenko, A. V. Konyashchenko, A. P. Lutsenko, and S. Yu. Tenyakov, "Contrast degradation in a chirped-pulse amplifier due to generation of prepulses by postpulses," Opt. Express 16, 3178-3190 (2008).

17. A. Jullien, O. Albert, F. Burgy, G. Hamoniaux, J.-P. Rousseau, J.-P. Chambaret, F. Au´ge-Rochereau, G. Cheriaux, J. Etchepare, N. Minkovski, and S. M. Saltiel, "$10^{-10}$ temporal contrast for femtosecond ultraintense lasers by cross-polarized wave generation," Opt. Lett. 30, 920–922 (2005).

18. C. Dorrer and J. Bromage, "Impact of high-frequency spectral phase modulation on the temporal profile of short optical pulses," Opt. Express 16, 3058-3068 (2008).

**19.** **http://www.ibsenphotonics.com/wp-content/uploads/White-paper-Fused-Silica-Transmission-Gratings-v1.0.pdf**

20. I. N. Ross, A. J. Langley, and P. Taday, "A Simple Achromatic Pulse Stretcher," Central Laser Facility Annual Report 1999/2000, 201-203 (2000).

221. O. E. Martinez, "3000 times grating compressor with positive group velocity dispersion: application to fiber compensation in 1.3-1.6-p~m region," IEEE J. Quantum Electron. QE-23, 59-64 (1987).

22. G. Cheriaux, P. Rousseau, F. Salin, J. P. Chambaret, B. Walker, and L.F. Dimauro, "Aberration-free stretcher design for ultrashort-pulse amplification," Opt. Lett. 21, 414 (1996).

23. M. Kalashnikov, A. Andreev, and H. Schönnagel, "Limits of the temporal contrast for CPA lasers with beams of high aperture," Proc. SPIE 7501, 750104 (2009).